Serveur Académique Lausannois SERVAL serval.unil.ch

Author Manuscript

Faculty of Biology and Medicine Publication

This paper has been peer-reviewed but does not include the final publisher proof-corrections or journal pagination.

Published in final edited form as:

Title: Development of a semi-automated image-based high-throughput drug screening system.

Authors: Eren RO, Kopelyanskiy D, Moreau D, Chapalay JB, Chambon M, Turcatti G, Lye LF, Beverley SM, Fasel N

Journal: Frontiers in bioscience (Elite edition)

Year: 2018 Jan 1

Issue: 10

Pages: 242-253

In the absence of a copyright statement, users should assume that standard copyright protection applies, unless the article contains an explicit statement to the contrary. In case of doubt, contact the journal publisher to verify the copyright status of an article.

serval
serveur académique lausannois

UNIL | Université de Lausanne
Faculty of Biology and Medicine

Development of a semi-automated image-based high-throughput drug screening system

Remzi Onur Eren[1], Dmitry Kopelyanskiy[1], Dimitri Moreau[2], Julien Bortoli Chapalay[3], Marc Chambon[3], Gerardo Turcatti[3], Lon-Fye Lye[4], Stephen M. Beverley[4], Nicolas Fasel[1]

[1]Department of Biochemistry, University of Lausanne, 1066 Epalinges, Switzerland,[2]Access Platform Swiss National Centre of Competence in Research (NCCR), University of Geneva, 1211 Geneva, Switzerland, [3]Biomolecular Screening Facility, Ecole Polytechnique Federale de Lausanne (EPFL), CH-1015 Lausanne, Switzerland, [4]Department of Molecular Microbiology, School of Medicine, Washington University, St. Louis, MO 63110, USA

TABLE OF CONTENTS

1. ABSTRACT

We previously reported that the innate sensing of the endosymbiont *Leishmania* RNA virus 1 (LRV1) within *Leishmania (Viannia) guyanensis* through Toll-like receptor 3, worsens the pathogenesis of parasite infection in mice. The presence of LRV1 has been associated with the failure of first-line treatment in patients infected with LRV1 containing -*L. guyanensis* and -*L. braziliensis* parasites. Here, we established a semi-automated image-based high-throughput drug screening (HTDS) protocol to measure parasiticidal activity of the Prestwick chemical library in primary murine macrophages infected with LRV1-containing *L. guyanensis*. The two-independent screens generated 14 hit compounds with over sixty-nine percent reduction in parasite growth compared to control, at a single dose in both screens. Our screening strategy offers great potential in the search for new drugs and accelerates the discovery rate in the field of drug repurposing against *Leishmania*. Moreover, this technique allows the concomitant assessment of the effect of drug toxicity on host cell number.

2. INTRODUCTION

Leishmania is an oblige intracellular protozoan parasite, which gives rise to a sand fly borne disease named leishmaniasis. Leishmaniasis may lead to symptomatic or asymptomatic primary cutaneous lesions at the site of inoculation. In addition to cutaneous lesions, *Leishmania Viannia* subgenus parasites can cause the metastatic types of leishmaniasis, namely mucocutaneous (MCL) and disseminated cutaneous (DCL) leishmaniasis (1). The underlying mechanism of metastatic leishmaniasis development remains largely unknown. Our previous studies show that the presence of an endosymbiotic double-stranded RNA (dsRNA) virus, in *L. guyanensis*, named Leishmania RNA virus 1 (LRV1), increases the disease severity and accelerates parasite dissemination in mice (2-4). Moreover, LRV1 leads to first-line treatment failure and symptomatic relapse of *L. guyanensis* and *L. braziliensis* infections in humans (5, 6).

Currently, no vaccination is available against leishmaniasis (7). There is a continuous and gradual increase in the prevalence of drug-resistant *Leishmania spp.* (8, 9). Current drug regimes against *Leishmania* parasites have severe side effects that can affect the quality of life of patients post-treatment. Furthermore, some treatment schemes require hospitalization, or trained personnel for intravenous administration (10-12). Thus, new drugs against leishmaniasis are required.

Promastigote or axenic amastigote *Leishmania* parasites have previously been used in drug discovery studies (13). Although promastigotes are easy to culture and handle in a laboratory setting, parasites at this stage represent the vector-

transmitted form of a parasite life cycle and do not biologically reflect intra-macrophage amastigotes. Moreover, the susceptibility of promastigotes and amastigotes to compounds may vary greatly (14). Thus, many potential anti-leishmanial compounds may be discarded during the initial screening against promastigotes due to their low parasiticidal activity. Axenic amastigotes on the other hand closely mimic the intracellular stage of the parasites, however, the host cell environment cannot be mimicked with these parasites (15). The interaction between the host cell and parasites is a crucial determining factor in the cellular fitness of parasites, this parameter should thus be taken into account when screening for new compounds.

Macrophages are the terminal host of the *Leishmania* parasite (16). Thus, primary murine macrophages are a good cell model to mimic intracellular infection and are easy to produce in large quantities. These primary cells enable adequate assessment of potential compounds for anti-parasitic efficacy as well as toxicity to the host-cell (17, 18). The drawback of using an *in vitro* macrophage infection model is the laborious, bias, and error-prone manual counting technique that is used to calculate the parasiticidal activity of drugs by counting intracellular amastigotes within cells.

Here, we introduced the method for an unbiased semi-automated image-based high-throughput drug screening (HTDS) against LRV1-bearing *L. guyanensis* within primary murine macrophages. We first optimized the *in vitro* conditions and developed an experimental pipeline, suitable for large-scale drug screening assays. We validated the method by evaluating the activity of the widely used anti-leishmanial drugs, namely amphotericin B and miltefosine. We subsequently screened the Prestwick chemical library using our established HTDS protocol.

MATERIALS AND METHODS

Ethical statement

The animal protocol used in this study was approved by the Swiss Federal Veterinary Office (SFVO), under the authorization numbers 2113.1. and 2113.2. Animal handling and experimental procedures were undertaken in accordance with ethical guidelines determined by the SFVO and under inspection by the Department of Security and Environment of the State of Vaud, Switzerland.

Bone-marrow derived macrophage production

Tibias and femurs of naive C57BL/6 mice were washed with complete DMEM containing 10 percent FBS, 1 percent penicillin/streptomycin, and 1 percent HEPES to collect bone marrow. Cell suspensions were then filtered through a 40-micrometer filter and centrifuged at 200xg for 8 minutes at 4 degrees Celsius. Cells were resuspended in complete DMEM, and then counted using a Vi-CELL Series Cell Viability Analyzer, and cultured with 50 ng/ml mouse recombinant macrophage colony stimulating factor (M-CSF) at a concentration of $7x10^5$ cells/ml for 6 days. 5 ml complete DMEM supplemented with 50 ng/ml rMCSF was added after 3 days of culture. On the sixth day, the medium was aspirated and cells were washed with ice-cold 1xPBS, pH 7.4. containing 5mM EDTA to detach the cells.

Flow cytometry analysis of bone-marrow derived macrophages

Cells were resuspended in 100 microliter of staining solution, containing an equal amount of FACS buffer (1xPBS with 2 percent FBS) and 24G2 conditioned medium. Cells were stained with anti-CD11b and anti-F4/80 antibodies for 30 minutes. Samples were then washed with FACS buffer. FACS analysis was performed using a BD Accuri C6 or BD LSRII cytometer and analyzed in FlowJo (v9.7.5., TreeStar), or BD FACSDiva software.

In vitro parasite culture

LRV1 containing *L. guyanensis* (MHOM/BR/75/M4147) were used in this study. Promastigotes were cultured with Schneider's insect medium supplemented with 20 percent heat-inactivated FBS and 50U/ml penicillin/streptomycin. Parasites were cultured at 26 degrees Celsius with 5 percent CO_2 supply for 5-6 days. Stationary stat-phase promastigotes were used to infect macrophages.

The plating and infection of macrophages

100 microliters of macrophage suspension at a concentration $1.2.5x10^6$ cells/ml were supplemented with 50 ng/ml of rMCSF and dispensed into clear-bottom 96-well plates using a Multidrop Combi Reagent Dispenser. Assay plates were then incubated at 37 degrees Celsius with a 5 percent CO_2 supply overnight. Stationary promastigotes were centrifuged at 2000xg for 10 min at room temperature. Parasites were resuspended in complete DMEM, and were counted using a counting chamber. Parasite concentration was adjusted to $12.5.x10^6$ cells/ml in complete DMEM, supplemented with 50 ng/ml of rMCSF. 100 microliters of promastigotes at a multiplicity of infection (MOI) of 10 were dispensed on top of macrophages using a Multidrop Combi Reagent Dispenser. Macrophages were incubated with parasites at 35 degrees Celsius with a 5 percent CO_2 supply for 48 hours. Cells were dispensed at the fine edge of the well to have a homogenous distribution of cells.

3.6. Drug library preparation

The Prestwick chemical library (PCL) was divided into sixteen assay plates. Tested compounds and controls were echo-dispensed by Echo 550 (Labcyte), located in the Biomolecular screening facility (BSF) of the Ecole Polytechnique Fédérale de

Lausanne (EPFL). All compounds together with positive and negative controls were echo-dispensed into plates. The plates were then were stored at -20degrees Celsius.

3.7. Compound library administration

The compound plates were thawed and briefly centrifuged. Preheated complete DMEM was dispensed into wells using a Multidrop Combi Reagent Dispenser. Compound plates were then shook, briefly centrifuged, and aspirated using a Bravo Automated Liquid Handling Platform and dispensed on the middle of corresponding wells. All compounds were assayed at 10 micromolar in this screening method. Plates were incubated at 35 degrees Celsius with a 5 percent CO_2 supply for an additional 48 hours.

3.8. Staining and image acquisition

Cells were subsequently fixed with freshly-made 4 percent paraformaldehyde (PFA) pH 7.4., for 15 minutes, pH 7.4., washed with 1xPBS then stained with DAPI (Molecular Probe®) and phalloidin-Alexa488 (Molecular Probe®) in 1xPBS using a Bio-Tek plate washer. Images were acquired using a 40x air-lens with a high content microscope. 49 square images of 352.0.8 x 352.0.8 micrometer size and 200 micrometer distance between them were taken in each well. MetaXpress and AcquityEpress software were used for image acquisition processing and consequent analysis.

RESULTS

The screening method was based on primary macrophages that were infected with *L. guyanensis* promastigotes at stationary phase. We used a well-established method to produce macrophages by incubating murine bone-marrow progenitors with macrophage-colony stimulating factor (M-CSF). As previously described, plated macrophages were incubated with medium containing M-CSF to enhance the cellular fitness of these primary cells during the screening (19). Current image-based drug screening assays require an additional wash step in order to remove the excess promastigotes that stayed extracellularly following *in vitro* infection. We found that the promastigotes of *L. major*, but not *L. guyanensis* and *L. braziliensis* parasites, survived at 35 degrees Celsius (data not shown). Thus, macrophages were not washed after the infection. Consequently, we adapted and modified the previously established screening protocol of Aulner *et al* (Figure 1A) (19). To ensure the complete transition of intracellular promastigotes to amastigotes, macrophages were incubated with promastigote for two days. The time window for drug incubation was reduced from three to two days in order to increase the cell count in our assay. The pipeline of the screening assay comprised the dispensation of cells, parasites and drugs. Therefore, our pipeline included manual handling of assay plates during automated cell dispensing, automated plate washing, and automated compound pipetting. The time outside the cell incubator for the assay plates during these steps was less than one minute per plate for parasite and cell dispensation, and three minutes per four plates for compound dispensation.

To detect intracellular amastigote and macrophage nuclei, we used DAPI, a fluorescent DNA intercalating dye. The nuclei of macrophages and parasites were segmented according to their size (Figure 1B). Heterochromatin regions of macrophage nucleus could wrongly be segmented as parasite nuclei by the software. To overcome this issue, macrophage nuclei were subtracted from the raw image after cell segmentation (Figure 1B). We excluded cells having nuclear stain but lacking cytoplasmic stain, and omitted the count of fragmented nuclei debris by setting size and shape restrictions (Figure 1B). Parasites that were within the boundaries of the macrophage cytoplasm were counted (Figure 1C). To increase sensitivity for the parasite and macrophage ratio calculation, cells that were located on the image boundaries were excluded (Figure 1C and 1D).

Assay optimization

We initially performed experiments to identify the optimal M-CSF concentration. The desired concentration would lead to macrophage survival, resulting in similar macrophage count in both infected and non-infected conditions without causing cell stacking. Our data showed that 50 ng/ml of M-CSF was enough to maintain an adequate macrophage number, and did not lead to discrepancies in cell number during parasite infection (Figure 2A and 2B). However, the addition of lower or higher concentrations of M-CSF leads to low cell yield and cell stacking, respectively (Figure 2A and 2B). We subsequently tested various MOI ratios to decipher an optimal parameter that results in a high infection rate and yields a similar cell count compared to non-infected controls (Figure 2C). These criteria were satisfied with a MOI of 10.

Assay verification with reference compounds

To test and validate the screening assay for its pharmacological relevance, we measured the half-maximal effective concentration (EC50) of two widely used anti-parasiticidal drugs, amphotericin B and miltefosine. Our results demonstrated that miltefosine was toxic to primary macrophages at concentrations above 15 micromolar, while we observe cytotoxicity to a certain extent for amphotericin B at any tested concentrations (Figure 3A and 3B). The EC50 values for amphotericin B and miltefosine were 0.2.5 micromolar (plus or minus 0.0.6) and 4.1.0 micromolar (plus or minus 1.1.2), which coincide with previously published data (Figure 3A and 3B) (14, 17, 19-21).

Subsequently, we performed the HTDS protocol to measure the drug potency of miltefosine at 15 micromolar and amphotericin B at 1 micromolar using primary macrophages infected with LRV1-containing *L. guyanensis* parasites at various MOI. We found that the parasite per macrophage ratio was drastically different between vehicle control and drug-treated infected cells at a MOI of 10 (Figure 3C and 3D). Amphotericin B was used as a reference drug in the screening assay due to its consistent nanomolar range parasiticidal activity in other image-based drug screening assays.

Drug screening

We performed two independent HTDS screens against LRV1-containing *L. guyanensis* using a Prestwick chemical library. The screen has a 1.0.9% yield. Two infection experiments were performed with parasites isolated independently from the footpads of infected mice, and these parasite isolates were used in the HTDS procedure. The Z′-factor for each plate was over 0.5. (data not shown), indicating the robustness of the assay. The parasite counts of amphotericin B-treated infected and non-infected macrophages were similar, and were distinctly different from the parasite counts of DMSO-treated infected macrophages (Figure 4A). The cell number of non-infected macrophages in wells from two-independent experiments was closely similar or identical (Figure 4B). Macrophage number together with parasite number varied between experiments (Figure 4B), however the infection ratio remained similar (data not shown). We identified fourteen compounds with parasiticidal activity of over 69 percent and over 75 percent on average in two-independent screens (Table 1). A secondary validation screen was undertaken to measure the EC50 of identified compounds (Figure 4C). We found that all compounds displayed an anti-parasiticidal activity of over 65% at a 10 micromolar concentration, except dequalinium dichloride, sulconazole nitrate, tioconazole and oxiconozole nitrate (Figure 4C). Our data showed that antimycin A and disulfiram had parasiticidal potency at the nanomolar range without cellular toxicity.

DISCUSSION

In this study, we established a semi-automated high-throughput image-based drug screening technique in *L. guyanensis* LRV1-bearing infected macrophages considering the potential impact of LRV1 on treatment failure and relapses. The HTDS method offers unbiased, quantitative and statistical-powerful data. High-content based methods drastically reduced the duration of the primary drug screening procedure for leishmaniasis. The limitation in the HTDS method against *Leishmania* promastigotes is an additional washing step to remove excess extracellular promastigotes. We found that *L. guyanensis*, but not *L. major*, promastigotes were temperature sensitive, and could not survive outside of macrophages at 35 degrees Celsius. This feature of *L. guyanensis* facilitated the liquid handling in our HTDS protocol. Parasites were not transfected to express a fluorescent marker for detection in this protocol. The genetic alteration of parasites could require culturing with selection antibiotic for post-transfection selection, which can interfere with drug screening analysis (20). We showed that DAPI staining was sufficient for detection of both parasite and macrophage nuclei. Moreover, cytosolic staining of macrophages allowed the quantification of intracellular amastigotes at the single cell level. The exclusion of cells with a cytosol stretching beyond the area of sight allowed us to have a more accurate parasite per macrophage ratio.

We identified two drugs, disulfiram and antimycin A, with submicromolar anti-parasitic activity. Disulfiram is a lipophilic compound with a high octanol/water partition coefficient, facilitating lipid membrane permeability and increasing the bioavailability of drugs to amastigotes within the phagolysosome of macrophages. The inhibition of superoxide dismutase by disulfiram can also contribute to its high parasiticidal activity (22). Consistent with our results, a study identified disulfiram as a parasitoxic compound using promastigote based screening, and verified its potency using axenic amastigotes. However, the *in vivo* activity of disulfiram was relatively low, even though the drug treatment of mice started 3 days post infection. Disulfiram also displays a growth inhibitory effect against other parasites including *Plasmodium falciparum* (23),, *Trichomonas vaginalis* (24) and *Tritrichomonas foetus* (24). The metabolic byproduct of disulfiram has a metal chelator function, which can decrease the nephrotoxicity of platinum-based cisplatin in the combinational drug treatment of trypanosomiasis (25). It would be interesting to investigate the effects of disulfiram treatment in metal-based therapeutics for leishmaniasis.

Antimycin A is an inhibitor of the mitochondrial complex III, and was reported to be parasitotoxic to *L. donovani* and *L. mexicana* parasites at nanomolar concentrations (20, 25). The inhibition of electron transport in the mitochondrial respiratory chain induces reactive oxygen species production (26). Thus, the treatment by antimycin A can enhance macrophage-mediated killing of parasites. A point mutation in the apocytochrome b gene of a *L. tarentole* parasite strain was associated to antimycin A-resistance (27). This finding indicates that the therapeutical potency of antimycin A given to the possible emergence of drug-resistant parasites.

Some other identified compounds have been reported to have antiparasitic activity. Astemizole, a known H1-histidine receptor antagonist, has been shown to inhibit proliferation of 3 different strains of *P. falciparum* that differ in their sensitivity to common antimalarial drugs (28). Bepridil hydrochloride is a calcium channel protein inhibitor that was shown to be parasitotoxic against various species of *Leishmania in vitro* but not *in vivo* (29). Dequalinium dichloride is an anti-microbial antiseptic medication with a large spectrum of bactericidal and fungicidal activity. In combination with chloroquine, dequalinium dichloride was shown to be an efficient antimalarial agent (30), and displayed some mild activity against *Trypanosoma brucei* (31). Mefloquine hydrochloride is a medication used to prevent malaria. However, mefloquine hydrochloride was inactive against *Leishmania amazonensis in vivo* (32). One of the hits is pentamidine isethionate, which is a well-known anti-leishmanial drug

(33). Two azole-containing antifungal compounds including oxiconazole nitrate and tioconazole were reported to have leishmaniacidal activity *in vitro (34, 35)*.

In summary, the drug discovery process using HTDS allowed us to take into consideration two crucial parameters in parasite infection, namely the biology of the host cell and the interaction between host cells and parasites. This is relevant considering that drugs can have an indirect anti-parasitic effect by augmenting anti-parasiticidal activity of host cells, and can require the host cell metabolic processing to be active. Moreover, the concurrent analysis of drug-toxicity on host cells facilitates the hit identification, and the usage of genetically untouched parasites in the screening reduces the risk of data misinterpretation. This methodology is superior to classical drug screening techniques and presents a great potential for high-throughput drug screening against *Leishmania* parasites.

ACKNOWLEDGEMENTS

Remzi Onur Eren and Dmitry Kopelyanskiy contributed equally to this paper. We are thankful to Cansel Ustunel Eren for her assistance with the high-content microscopy and to Slavica Masina for critical reading of the manuscript. We thank the NCCR Access platform for providing the equipment for the high-content microscope experiments and drug library. Conceptualization R.O.E. and N.F; Methodology R.O.E and N.F; Investigation R.O.E., D.K. and N.F; Resources D.M., J.B.C., M.C., G.T., L-F.L and S.M.B; Writing - Original Draft R.O.E., D.K., and N.F; Writing- Review & Editing R.O.E., D.K., and N.F; Funding Acquisition R.O.E. and N.F. This work is funded by grants from the COST action (CM1307 SEFRI: C14.0.070, N.F.), the Swiss National fund for research (FNRS 310030-153204 and IZRJZ3_164176,N.F.) and by NIH Grants (R01AI029646 and R56AI099364 to S.M.B.).

REFERENCES

1. M. A. Hartley, C. Ronet, H. Zangger, S. M. Beverley and N. Fasel: Leishmania RNA virus: when the host pays the toll. *Front Cell Infect Microbiol*, 2, 99 (2012)
2. A. Ives, S. Masina, P. Castiglioni, F. Prevel, M. Revaz-Breton, M. A. Hartley, P. Launois, N. Fasel and C. Ronet: MyD88 and TLR9 dependent immune responses mediate resistance to Leishmania guyanensis infections, irrespective of Leishmania RNA virus burden. *PLoS One*, 9(5), e96766 (2014)
3. A. Ives, C. Ronet, F. Prevel, G. Ruzzante, S. Fuertes-Marraco, F. Schutz, H. Zangger, M. Revaz-Breton, L. F. Lye, S. M. Hickerson, S. M. Beverley, H. Acha-Orbea, P. Launois, N. Fasel and S. Masina: Leishmania RNA virus controls the severity of mucocutaneous leishmaniasis. *Science*, 331(6018), 775-8 (2011)
4. M. A. Hartley, E. Bourreau, M. Rossi, P. Castiglioni, R. O. Eren, F. Prevel, P. Couppie, S. M. Hickerson, P. Launois, S. M. Beverley, C. Ronet and N. Fasel: Leishmaniavirus-Dependent Metastatic Leishmaniasis Is Prevented by Blocking IL-17A. *PLoS Pathog*, 12(9), e1005852 (2016)
5. V. Adaui, L. F. Lye, N. S. Akopyants, M. Zimic, A. Llanos-Cuentas, L. Garcia, I. Maes, S. De Doncker, D. E. Dobson, J. Arevalo, J. C. Dujardin and S. M. Beverley: Association of the Endobiont Double-Stranded RNA Virus LRV1 With Treatment Failure for Human Leishmaniasis Caused by Leishmania braziliensis in Peru and Bolivia. *J Infect Dis*, 213(1), 112-21 (2016)
6. E. Bourreau, M. Ginouves, G. Prevot, M. A. Hartley, J. P. Gangneux, F. Robert-Gangneux, J. Dufour, D. Sainte-Marie, A. Bertolotti, F. Pratlong, R. Martin, F. Schutz, P. Couppie, N. Fasel and C. Ronet: Presence of Leishmania RNA Virus 1 in Leishmania guyanensis Increases the Risk of First-Line Treatment Failure and Symptomatic Relapse. *J Infect Dis*, 213(1), 105-11 (2016)
7. P. M. Gillespie, C. M. Beaumier, U. Strych, T. Hayward, P. J. Hotez and M. E. Bottazzi: Status of vaccine research and development of vaccines for leishmaniasis. *Vaccine*, 34(26), 2992-5 (2016)
8. S. L. Croft, S. Sundar and A. H. Fairlamb: Drug resistance in leishmaniasis. *Clin Microbiol Rev*, 19(1), 111-26 (2006)
9. A. S. Nagle, S. Khare, A. B. Kumar, F. Supek, A. Buchynskyy, C. J. Mathison, N. K. Chennamaneni, N. Pendem, F. S. Buckner, M. H. Gelb and V. Molteni: Recent developments in drug discovery for leishmaniasis and human African trypanosomiasis. *Chem Rev*, 114(22), 11305-47 (2014)
10. S. Sundar and J. Chakravarty: Liposomal amphotericin B and leishmaniasis: dose and response. *J Glob Infect Dis*, 2(2), 159-66 (2010)
11. T. P. Dorlo, M. Balasegaram, J. H. Beijnen and P. J. de Vries: Miltefosine: a review of its pharmacology and therapeutic efficacy in the treatment of leishmaniasis. *J Antimicrob Chemother*, 67(11), 2576-97 (2012)
12. Ashutosh, S. Sundar and N. Goyal: Molecular mechanisms of antimony resistance in Leishmania. *J Med Microbiol*, 56(Pt 2), 143-53 (2007)
13. D. Sereno, A. Cordeiro da Silva, F. Mathieu-Daude and A. Ouaissi: Advances and perspectives in Leishmania cell based drug-screening procedures. *Parasitol Int*, 56(1), 3-7 (2007)
14. J. L. Siqueira-Neto, S. Moon, J. Jang, G. Yang, C. Lee, H. K. Moon, E. Chatelain, A. Genovesio, J. Cechetto and L. H. Freitas-Junior: An image-based high-content screening assay for compounds targeting intracellular Leishmania donovani amastigotes in human macrophages. *PLoS Negl Trop Dis*, 6(6), e1671 (2012)

15. A. Rochette, F. Raymond, J. Corbeil, M. Ouellette and B. Papadopoulou: Whole-genome comparative RNA expression profiling of axenic and intracellular amastigote forms of Leishmania infantum. *Mol Biochem Parasitol*, 165(1), 32-47 (2009)
16. E. Handman and D. V. Bullen: Interaction of Leishmania with the host macrophage. *Trends Parasitol*, 18(8), 332-4 (2002)
17. M. De Rycker, I. Hallyburton, J. Thomas, L. Campbell, S. Wyllie, D. Joshi, S. Cameron, I. H. Gilbert, P. G. Wyatt, J. A. Frearson, A. H. Fairlamb and D. W. Gray: Comparison of a high-throughput high-content intracellular Leishmania donovani assay with an axenic amastigote assay. *Antimicrob Agents Chemother*, 57(7), 2913-22 (2013)
18. M. Vermeersch, R. I. da Luz, K. Tote, J. P. Timmermans, P. Cos and L. Maes: In vitro susceptibilities of Leishmania donovani promastigote and amastigote stages to antileishmanial reference drugs: practical relevance of stage-specific differences. *Antimicrob Agents Chemother*, 53(9), 3855-9 (2009)
19. N. Aulner, A. Danckaert, E. Rouault-Hardoin, J. Desrivot, O. Helynck, P. H. Commere, H. Munier-Lehmann, G. F. Spath, S. L. Shorte, G. Milon and E. Prina: High content analysis of primary macrophages hosting proliferating Leishmania amastigotes: application to anti-leishmanial drug discovery. *PLoS Negl Trop Dis*, 7(4), e2154 (2013)
20. M. J. Dagley, E. C. Saunders, K. J. Simpson and M. J. McConville: High-content assay for measuring intracellular growth of Leishmania in human macrophages. *Assay Drug Dev Technol*, 13(7), 389-401 (2015)
21. E. Morais-Teixeira, Q. S. Damasceno, M. K. Galuppo, A. J. Romanha and A. Rabello: The in vitro leishmanicidal activity of hexadecylphosphocholine (miltefosine) against four medically relevant Leishmania species of Brazil. *Mem Inst Oswaldo Cruz*, 106(4), 475-8 (2011)
22. M. Marikovsky, V. Ziv, N. Nevo, C. Harris-Cerruti and O. Mahler: Cu/Zn superoxide dismutase plays important role in immune response. *J Immunol*, 170(6), 2993-3001 (2003)
23. L. W. Scheibel, A. Adler and W. Trager: Tetraethylthiuram disulfide (Antabuse) inhibits the human malaria parasite Plasmodium falciparum. *Proc Natl Acad Sci U S A*, 76(10), 5303-7 (1979)
24. M. J. Bouma, D. Snowdon, A. H. Fairlamb and J. P. Ackers: Activity of disulfiram (bis(diethylthiocarbamoyl)disulphide) and ditiocarb (diethyldithiocarbamate) against metronidazole-sensitive and -resistant Trichomonas vaginalis and Tritrichomonas foetus. *J Antimicrob Chemother*, 42(6), 817-20 (1998)
25. G. De Muylder, K. K. Ang, S. Chen, M. R. Arkin, J. C. Engel and J. H. McKerrow: A screen against Leishmania intracellular amastigotes: comparison to a promastigote screen and identification of a host cell-specific hit. *PLoS Negl Trop Dis*, 5(7), e1253 (2011)
26. Q. Chen, E. J. Vazquez, S. Moghaddas, C. L. Hoppel and E. J. Lesnefsky: Production of reactive oxygen species by mitochondria: central role of complex III. *J Biol Chem*, 278(38), 36027-31 (2003)
27. A. Schnaufer, S. Sbicego and B. Blum: Antimycin A resistance in a mutant Leishmania tarentolae strain is correlated to a point mutation in the mitochondrial apocytochrome b gene. *Curr Genet*, 37(4), 234-41 (2000)
28. C. R. Chong, X. Chen, L. Shi, J. O. Liu and D. J. Sullivan, Jr.: A clinical drug library screen identifies astemizole as an antimalarial agent. *Nat Chem Biol*, 2(8), 415-6 (2006)
29. J. Q. Reimao, F. A. Colombo, V. L. Pereira-Chioccola and A. G. Tempone: In vitro and experimental therapeutic studies of the calcium channel blocker bepridil: detection of viable Leishmania (L.) chagasi by real-time PCR. *Exp Parasitol*, 128(2), 111-5 (2011)
30. J. R. Rodrigues and N. Gamboa de Dominguez: Plasmodium berghei: in vitro and in vivo activity of dequalinium. *Exp Parasitol*, 115(1), 19-24 (2007)
31. D. C. Jones, I. Hallyburton, L. Stojanovski, K. D. Read, J. A. Frearson and A. H. Fairlamb: Identification of a kappa-opioid agonist as a potent and selective lead for drug development against human African trypanosomiasis. *Biochem Pharmacol*, 80(10), 1478-86 (2010)
32. L. O. Galvao, S. Moreira Junior, P. Medeiros Junior, G. J. Lemos, N. F. Cunha, R. M. Antonino, B. S. Santos Filho and A. V. Magalhaes: Therapeutic trial in experimental tegumentary leishmaniasis caused by Leishmania (Leishmania) amazonensis. A comparative study between mefloquine and aminosidine. *Rev Soc Bras Med Trop*, 33(4), 377-82 (2000)
33. I. Hellier, O. Dereure, I. Tournillac, F. Pratlong, B. Guillot, J. P. Dedet and J. J. Guilhou: Treatment of Old World cutaneous leishmaniasis by pentamidine isethionate. An open study of 11 patients. *Dermatology*, 200(2), 120-3 (2000)
34. A. Gebre-Hiwot and D. Frommel: The in-vitro anti-leishmanial activity of inhibitors of ergosterol biosynthesis. *J Antimicrob Chemother*, 32(6), 837-42 (1993)
35. M. Kaiser, P. Maser, L. P. Tadoori, J. R. Ioset and R. Brun: Antiprotozoal Activity Profiling of Approved Drugs: A Starting Point toward Drug Repositioning. *PLoS One*, 10(8), e0135556 (2015)

Key Words: *Leishmania*, high-content microscope, drug screening

Send correspondence to: Nicolas Fasel, Department of Biochemistry, University of Lausanne, 1066 Epalinges, Switzerland , Tel: + 41 21 692 5732, Fax: 0041-21-6925705, E-mail: nicolas.fasel@unil.ch

Figure 1. The pipeline of assay and data analysis. (A) The outline of experimental workflow. Bone-marrow progenitors were obtained from C57/BL6 mice and were cultured with M-CSF containing complete cell media for six days. Cells were counted using an automated cell counter, and dispensed in cleared bottom 96-well plates using an automated cell dispenser. Plates were incubated in 37 degrees Celsius, 5 percent CO_2 incubator overnight, ensuring the adherence of macrophages. Stationary LRV1

containing *Leishmania guyanensis* promastigotes were cultured for 6 days and then dispensed on cells at MOI of 10. To increase the infection rate and boost the parasite growth, plates were cultured at 35 degrees Celsius, 5 percent CO_2 incubator for the rest of the experimental procedure. Two days subsequent to infection, drugs were dispensed to the wells using a robotic liquid handler. Cells were processed for high content microscope acquisition two days post drug-treatment using a plate washer with plate-stacking function and peristaltic pump: fixation with freshly made 4 percent PFA, pH 7.4.; washing with 1xPBS, pH 7.4.; and staining with DAPI and phalloidin. The image acquisition was performed using a high content microscope, and a robotic arm for plate gripping. (B) The nuclear image staining was converted to binary image, and cell nucleus was subtracted from this image to identify and define parasites. (C) Cell area was defined as the combination of nuclear and cytosolic staining in a binary image. The cells that had cytosol bordering the edges of image were removed. (D) The final processed image contained segmented objects including cytosol (yellow), cell nucleus (pink), and parasite nuclei (blue).

Figure 2. Optimization of cell culture conditions and infection. (A-B) In HTDS procedure, macrophages were cultured with various amount of MCSF ranging from 1.5.6 to 400 ng/ml with two-fold increments. (A) Image displayed phalloidin staining and forty-nine composite images from each well. (B) Cells were counted using an automated image analysis. Graph shows the total cell count in obtained images per well. (C) HTDS were performed with macrophages that were supplemented with 50ng/ml MCSF, and were infected with parasites at various MOI. Graph displays macrophage cell number on the left-axis, and parasite per macrophage ratio on the right-axis. Data displays one significant independent experiment with three biological replicates.

Figure 3. Reference drug optimization. Eight-point dose response curves of (A) Amphotericin B and (B) miltefosine were generated using the HTDS protocol. (C-D) HTDS protocol were performed, and macrophages were treated with vehicle control (DMSO), 15 micromolar miltefosine, or 1 micromolar amphotericin B. Graph is a representative of three independent experiments (A-B) or of one with three technical replicates (C-D).

Figure 4. Primary and secondary HTDS screening. (A) Plot of the average parasite number (Y-axis) in forty-nine images of controls from the two independent primary screenings. (B) Plot of the average parasite number (X-Axis) and average macrophage number (Y-axis) in forty-nine images of controls the two independent primary screenings. (C) Eight-point dose response curves of compounds that displayed over sixty nine percent anti-leishmanial activity in two independent screens.

Table 1. Compounds that displayed over sixty nine percent anti-parasitic activity in two independent HTDS

	Anti-Leishmanial Activity (percent %)	
Compounds	**1st HTDS**	**2nd HTDS**
Antimycin A	93.1.9	95.2.4
Astemizole	83.6.1	92.9.7
Bepridil hydrochloride	93.6.6	83.3.5
Ciclopirox ethanolamine	94.6.5	95.6.5
Clofilium tosylate	83.0.3	76.7.0
Dequalinium dichloride	80.5.3	69.6.3
Disulfiram	90.8.9	87.1.2
Mefloquine hydrochloride	93.1.4	69.8.3
Oxiconazole Nitrate	91.6.9	94.7.2
Pentamidine isethionate	84.1.1	81.0.0
Perospirone	91.8.5	91.8.5
Prenylamine lactate	94.5.5	89.1.8
Sulconazole nitrate	95.6.2	93.6.5
Tioconazole	94.4.5	96.0.3

Running title: Image-based drug screening against *Leishmania* parasite

Figure 1

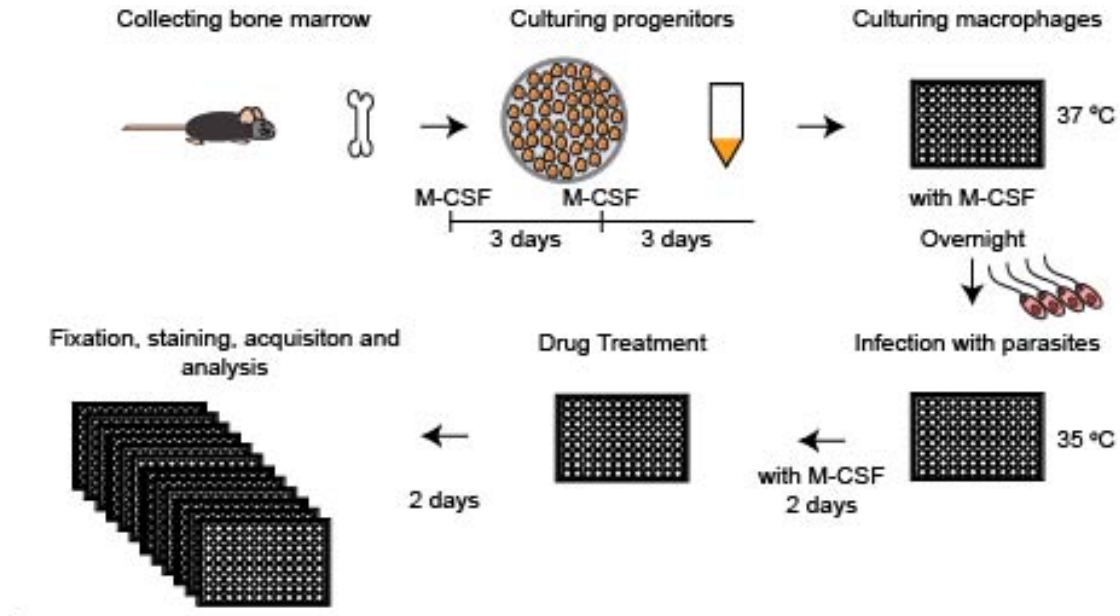

A

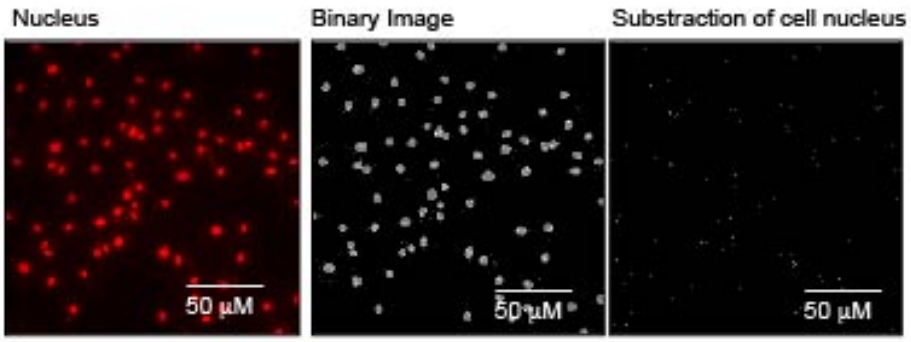

B

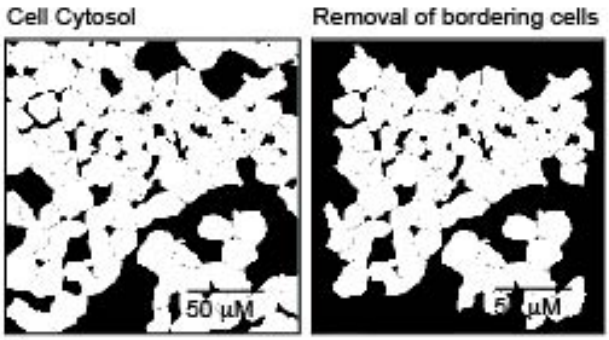

C

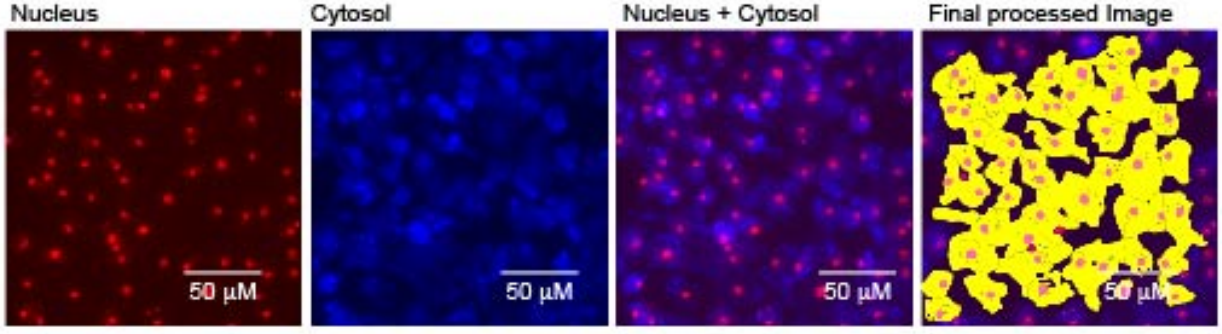

D

Figure 2

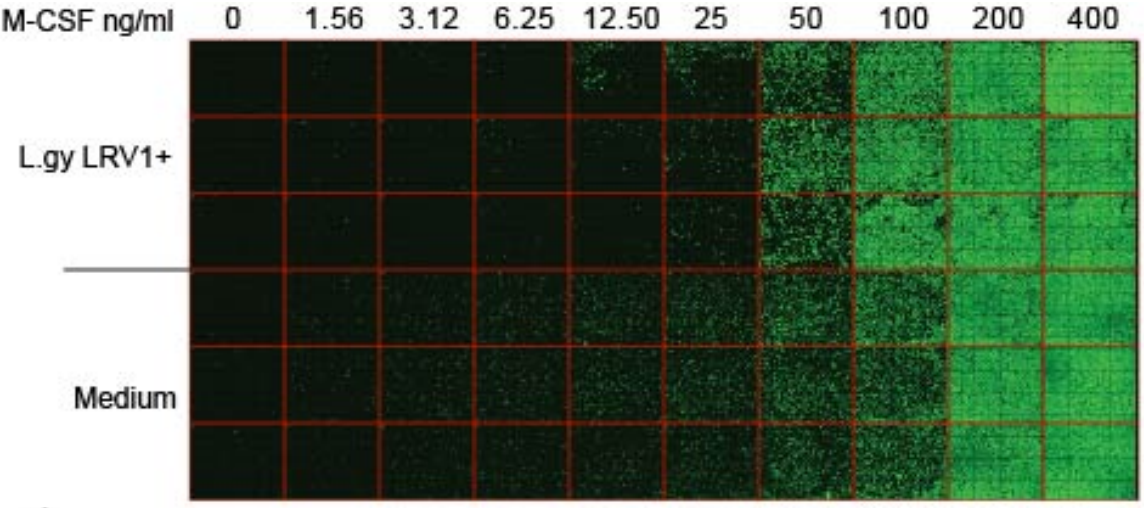
M-CSF ng/ml
0
1.56
3.12
6.25
12.50
25
50
100
200
400
L.gy LRV1+
Medium

A

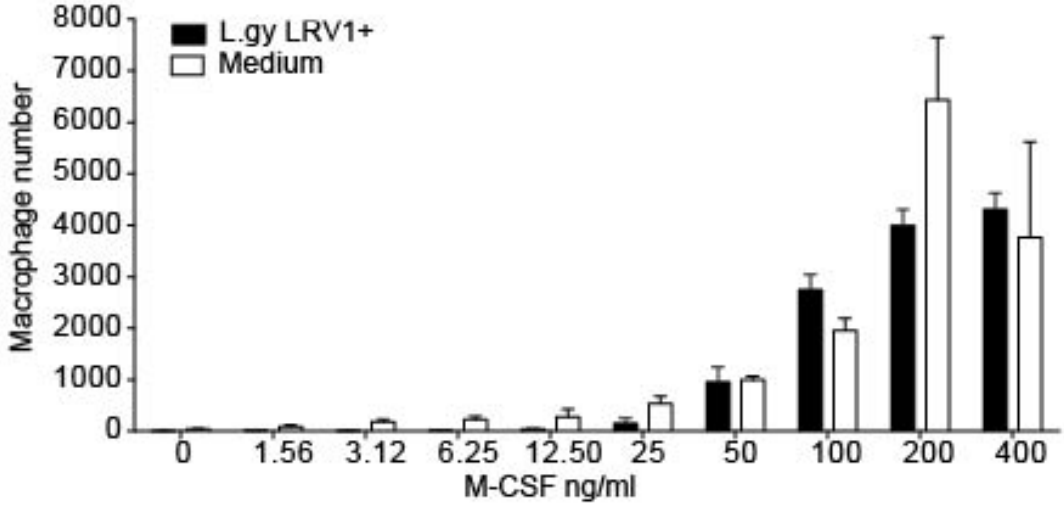
L.gy LRV1+
Medium
Macrophage number
8000
7000
6000
5000
4000
3000
2000
1000
0
0
1.56
3.12
6.25
12.50
25
50
100
200
400
M-CSF ng/ml

B

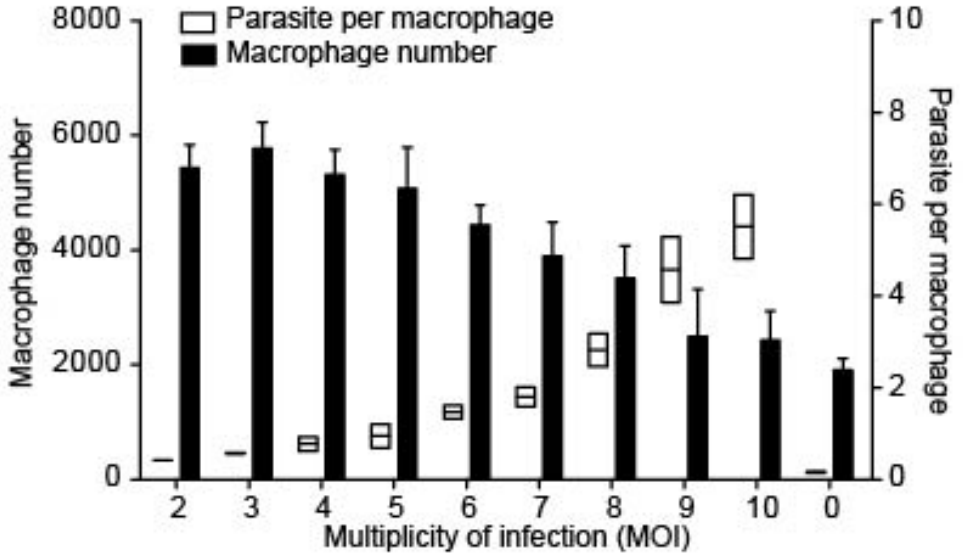
Parasite per macrophage
Macrophage number
Macrophage number
8000
6000
4000
2000
0
10
8
6
4
2
0
Parasite per macrophage
2
3
4
5
6
7
8
9
10
0
Multiplicity of infection (MOI)

C

Figure 3

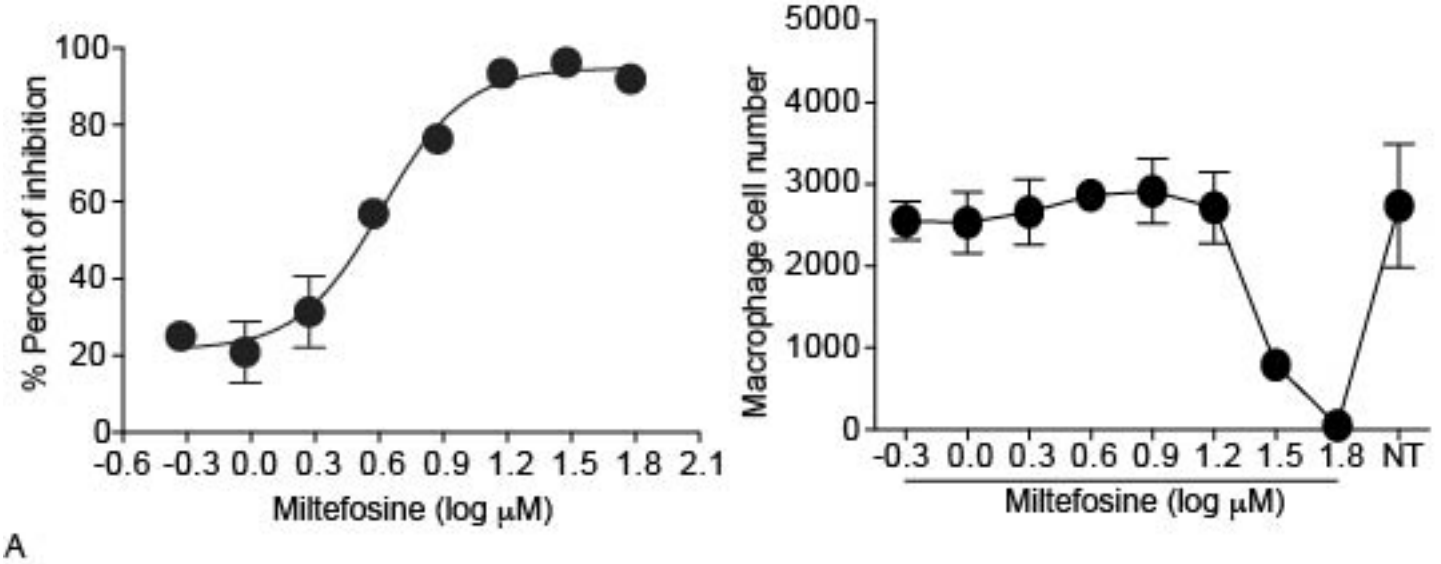

A

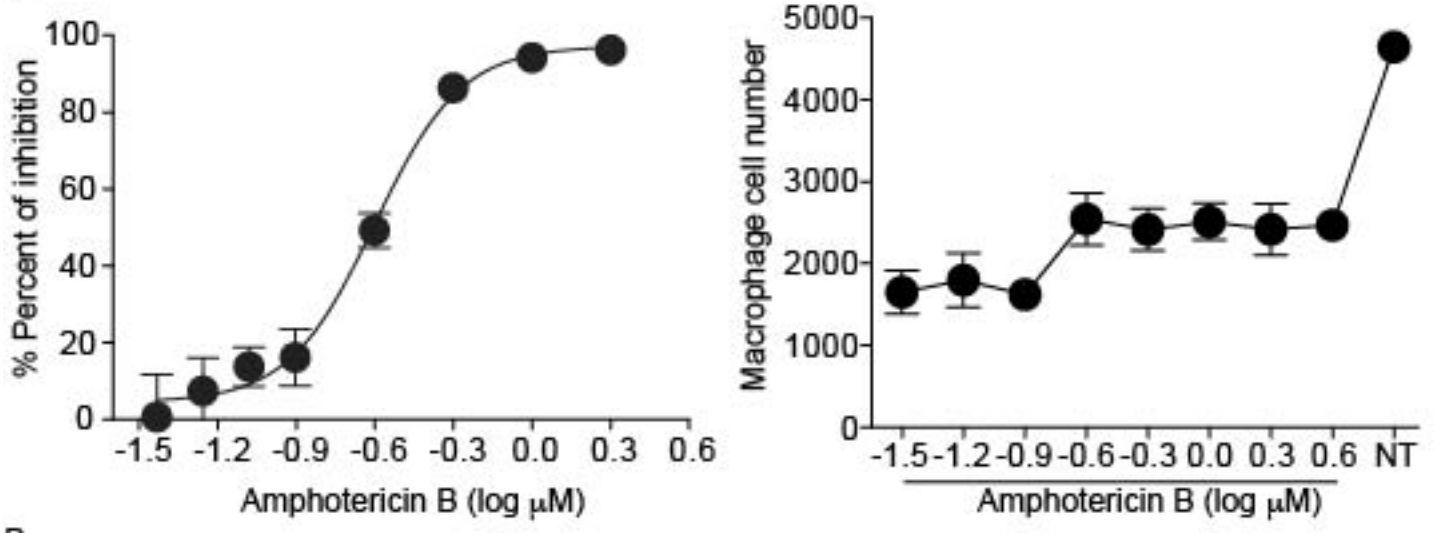

B

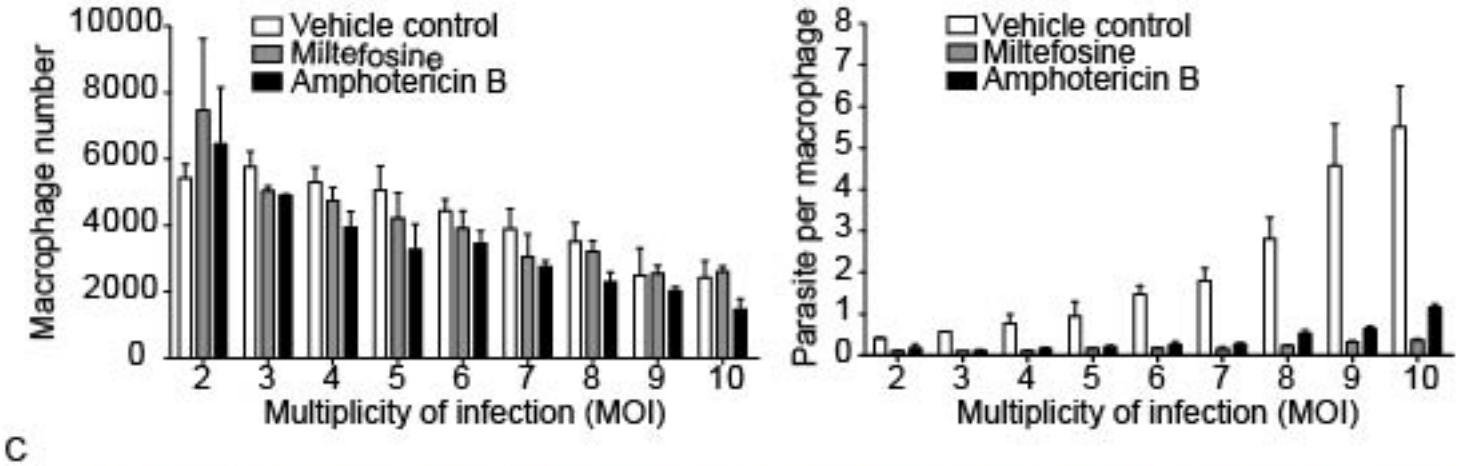

C

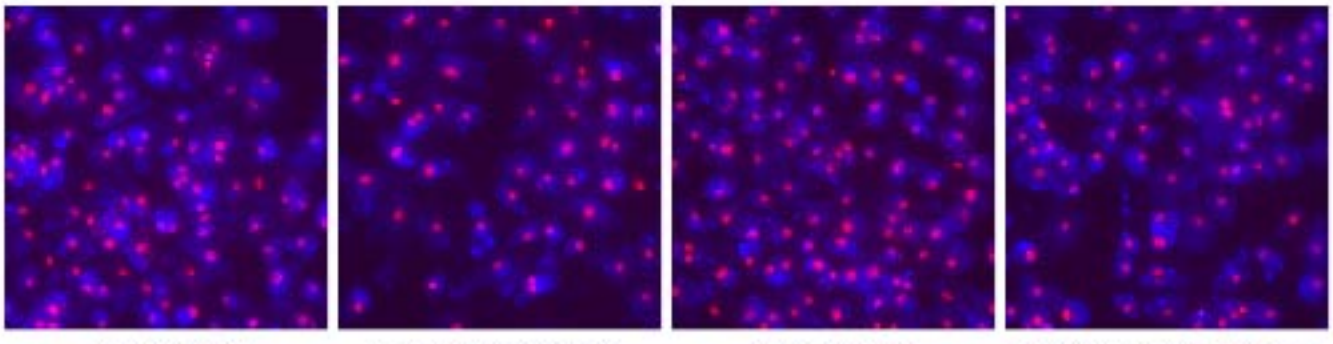

D

Figure 4

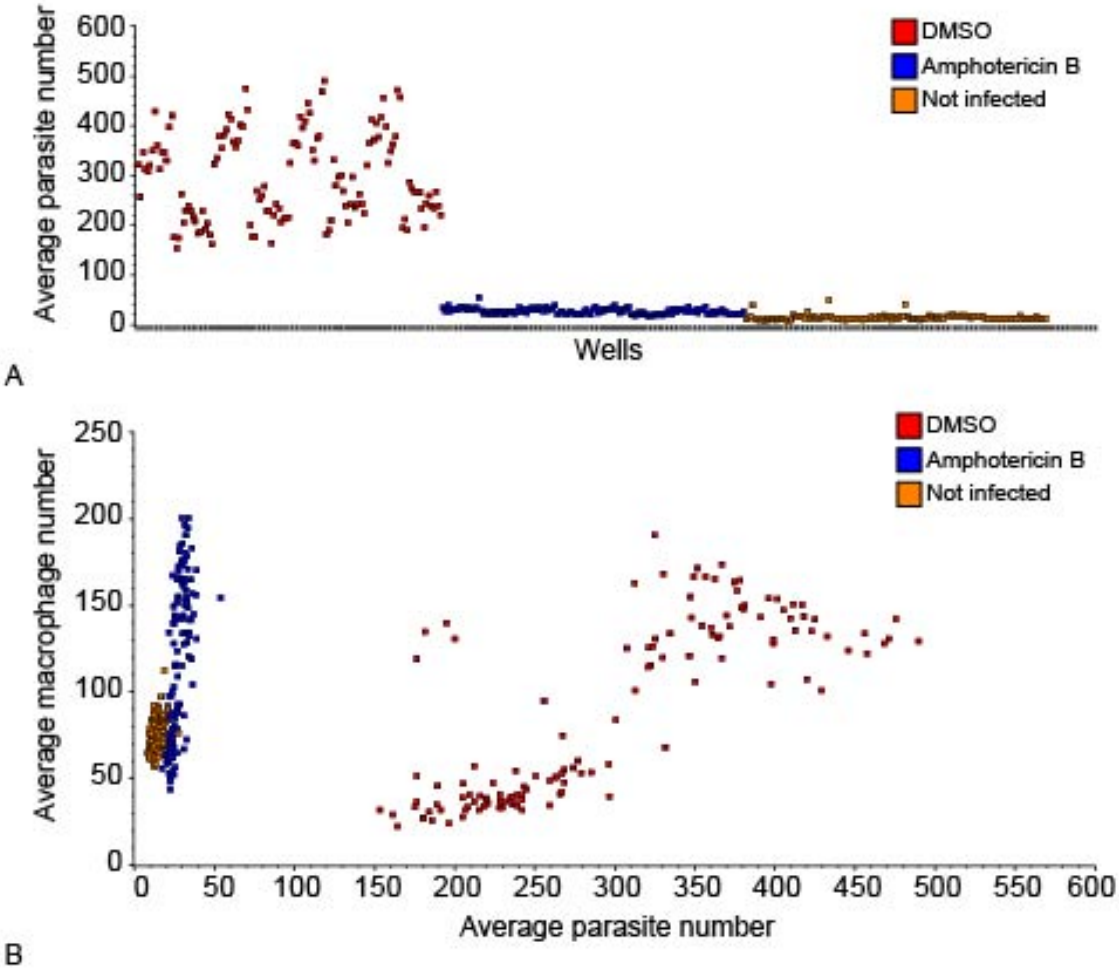
DMSO
Amphotericin B
Not infected
Average parasite number
Wells
A
Average macrophage number
Average parasite number
B
Antimycin A
Disulfiram
Astemizole
Bepridil hydrochloride
Ciclopirox ethanolamine
Clofilium tosylate
Dequalinium dichloride
Mefloquine hydrochloride
Oxiconazole Nitrate
Pentamidine isethionate
Perospirone
Prenylamine lactate
Sulconazole nitrate
Tioconazole
% Percent of inhibition
Concentration (log μM)
C